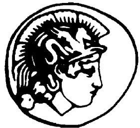

Pergamon

Acta Materialia 50 (2002) 643–651

www.elsevier.com/locate/actamat

Chemical ordering and texture in Ni–25 at% Al thin films

G.B. Thompson, R. Banerjee, X.D. Zhang, P.M. Anderson, H.L. Fraser *

Department of Materials Science and Engineering, The Ohio State University, Columbus, OH 43210, USA

Received 14 December 2000; received in revised form 28 August 2001; accepted 28 August 2001

Abstract

This paper describes a novel study of the microstructural development in sputter-deposited thin films from a target of the intermetallic compound Ni_3Al. Films were deposited on oxidized Si substrates at different temperatures, namely 45°C, 200°C, and 400°C. These films have been characterized by X-ray diffraction and transmission electron microscopy. In contrast to the behavior of sputter-deposited elemental metals and disordered alloys, the films deposited at the two higher temperatures consisted of refined microstructures and exhibited a low degree of texturing. This anomalous behavior has been explained by the role of exothermic heating accompanying chemical ordering. © 2002 Acta Materialia Inc. Published by Elsevier Science Ltd. All rights reserved.

Keywords: Sputtering; Thin films; Intermetallic compounds; Phase transformations (ordering); Recrystallization & recovery

1. Introduction

In recent years, thin film coatings have been of considerable interest for their potential use in high temperature aerospace applications. For example, thermal barrier coatings of Yittria stabilized Zirconia are used on turbine blades to help prevent oxidation of the base material. Besides providing oxidation protection, coatings may be used in areas requiring high temperature strength and creep resistance. The Ni_3Al or γ' phase is known to exhibit useful high temperature mechanical properties in the bulk form and these have lead to considerable research activities involving bulk Ni_3Al.

Regarding work aimed at exploring thin films of this intermetallic compound, some research groups have synthesized Ni–Al alloys in thin film form by thermal and electron beam evaporation. Harris and co-workers [1] deposited Ni_3Al thin films using high vacuum evaporation on polycrystalline copper substrates at room temperature as well as those cooled to 77 K. Nanocrystalline Ni–Al alloy films were prepared by vacuum evaporation on NaCl (001) substrates at temperatures in the range of 20–400°C [2]. Other studies have focused on the effect of irradiation on Ni–Al alloy thin films. For example, these include co-evaporation of Ni–Al films in the composition range of 18–23 at% Al by Alexander et al. [3] and the deposition of Ni/Al multilayers and subsequent ion-beam mixing of the multilayers by Eridon et al. [4]. The ion-beam mixing resulted in the formation of a number of metastable phases including an amorphous phase, a disordered crystalline phase and a hexagonal close-packed (h.c.p.) phase [4]. The formation of a meta-

* Corresponding author. Tel.: +1-614-292-2708; fax: +1-614-292-7523.

E-mail address: fraser.3@osu.edu (H.L. Fraser).

1359-6454/02/$22.00 © 2002 Acta Materialia Inc. Published by Elsevier Science Ltd. All rights reserved.
PII: S1359-6454(01)00373-1

stable h.c.p. phase has also been reported in irradiated co-evaporated Ni–Al alloy thin films [3]. There have also been a few studies on co-sputtered Ni–Al alloy thin films [5,6]. Cantor and Cahn [5] studied the formation of metastable alloy phases in co-sputtered alloy films in the composition range of 5–90 at% Ni (balance of Al). Films, 200–300 nm in thickness, were deposited by RF magnetron sputtering on liquid nitrogen cooled single crystal NaCl substrates. The results of TEM studies carried out by the authors on the as-deposited films indicate that while chemically disordered f.c.c. solid solutions formed for Al-rich and Ni-rich compositions, a disordered b.c.c. solid solution formed in the composition range 42.5–78.8 at% Ni. The lattice parameter of this disordered b.c.c. phase was 0.32 nm. Interestingly, in a more recent study on co-sputtered Ni–Al alloy thin films, Michaelson et al. [6] have reported the formation of the ordered B2 and an amorphous phase. The authors have studied Ni–Al films in the composition range 48–88 at% Al. Films, 2 μm thick, were deposited on sapphire substrates at room temperature. For a composition of 48 at% Al, the authors report the formation of a single chemically long range ordered B2 phase with a lattice parameter close to that of bulk B2 NiAl (a = 0.288 nm) [6]. For compositions richer than ~80 at% Al, the films exhibited a single disordered f.c.c. solid solution, while compositions in the range 60–75 at% Al formed a mixture of an amorphous phase and a crystalline phase. It is interesting to note that for the same nominal composition of ~50 at% Al, the results from the two studies indicate different results. Thus, while the film deposited at room temperature exhibited a single B2 phase [6], the film deposited on a liquid nitrogen cooled substrate exhibited a disordered b.c.c. phase with a substantially larger lattice parameter [5]. In this study, Ni_3Al thin films were deposited at three different substrate temperatures in order to understand the influence of this process parameter on the resultant microstructure.

2. Experimental procedure

Monolithic thin films of nominal composition Ni–25 at% Al were sputter deposited from an intermetallic Ni_3Al target using a custom built UHV magnetron sputtering unit. The substrates consisted of oxidized Si (100) wafers that had a 200 nm thick amorphous SiO_2 layer. The base pressure prior to sputtering was $\sim 5\times10^{-8}$ Torr and the argon pressure during sputtering was $\sim 2\times10^{-3}$ Torr. The nominal rate of deposition was 0.3 nm/s with the gun being power regulated at 200 W. As stated, the films were deposited at three different substrate temperatures, ~45°C (i.e. unheated), 200°C, and 400°C. A Ni_3Al intermetallic target with nominal composition was used for depositing the thin films. The thickness of the films in all cases was ~1 μm. The average composition of the films was measured using EDS in a scanning electron microscope and equals 75 at% Ni + 25 at% Al. X-ray diffraction experiments were conducted on the as-deposited films using a Scintag PAD V diffractometer. The X-ray tube was operated at 45 kV and 20 mA with CuK_α being the radiation (λ = 0.15406 nm). The scan rate was continuous at 1 degree per minute at a chopper increment of 0.03°. The films were also characterized by transmission electron microscopy (TEM) using a Philips CM200 operating at an accelerating voltage of 200 kV. Thin film specimens have been studied in both plan-view as well as cross-section geometries. The details of the sample preparation procedure are given elsewhere [7].

3. Results

In the present study, thin films of Ni–25Al have been deposited at three different substrate temperatures. To establish the baseline behavior expected from a simple f.c.c. metal, i.e., a high temperature metal with a crystallographically similar structure, Ni films were deposited at ambient and also at elevated temperatures (~600°C). The dominant texture in the films was {111} for both ambient as well as elevated temperature depositions. Both films exhibited a columnar grain morphology with the grain size being larger in the case of the film deposited at 600°C. The data is not presented here because it has been reported [8] that the degree of {111} texturing and the average grain size both increased upon increasing the substrate deposition

temperatures (up to ~550°C). The characterization of the Ni–25Al films is described in the following, and a comparison between the behavior of the simple metal and the intermetallic compound is made in the discussion section.

3.1. X-ray diffraction (XRD)

Fig. 1(a) is a plot of diffracted X-ray intensity vs. 2θ of the monolithic Ni–25Al film deposited on an unheated substrate. The presence of strong diffraction peaks indicates the formation of crystalline phases in this film. The most intense diffracted intensity occurs at $2\theta \approx 44°$, and as can be seen this intensity is provided by two nearly coincident

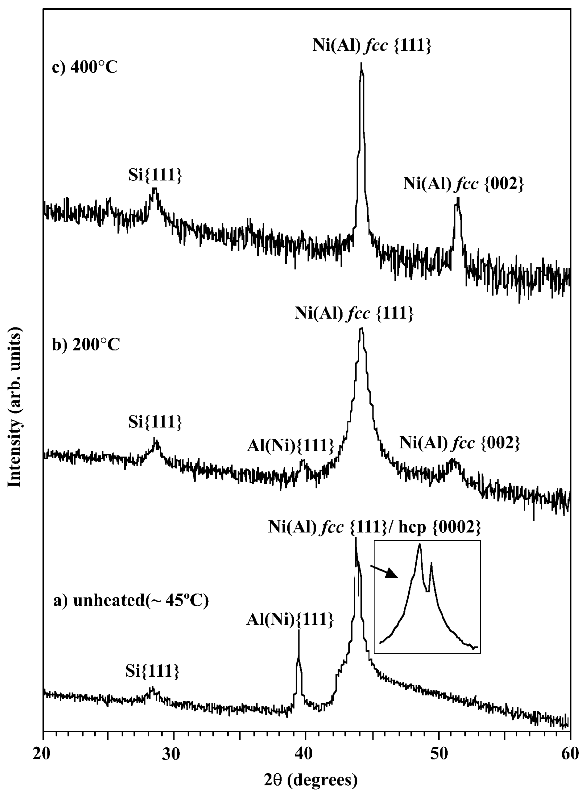

Fig. 1. XRD patterns from the Ni–25Al thin films deposited at (a) ~45°C, (b) 200°C and (c) 400°C. The {002} f.c.c. Ni(Al) peak progressively increases in intensity with increasing deposition temperatures suggesting the destruction of a strong ⟨111⟩ texture. The {111} Al(Ni) peak decreases in intensity with increasing deposition temperatures suggesting a reduction in the volume fraction of this metastable phase.

peaks. In the absence of other reflections, it is not possible to establish the identity of the crystal structure of the deposited phase(s). The most intense diffracted intensity occurs for a pair of split peaks at $2\theta = 43.85°$ and $2\theta = 44°$ which correspond to interplanar spacings of 0.2063 and 0.2056 nm, respectively. Thus, for example, the intensity maxima at $2\theta = 43.85°$ can be indexed as the {111} peak of an f.c.c. Ni(Al) phase with a lattice parameter of $a = 0.3573$ nm and the peak at $2\theta = 44°$ can be tentatively indexed as the {0002} peak of an h.c.p. Ni(Al) phase, with similar interplanar spacings of close packed planes. The absence of additional peaks from this phase suggests the presence of a high degree of texture in the as-deposited film. Further phase identification associated with these two peaks is discussed below in the TEM section. In addition to the intensity maximum referred to above, an additional peak is observed at $2\theta = 39.44°$. The interplanar spacing corresponding to this peak is 0.228 nm, which is similar to the {111} spacing for pure Al, i.e., 0.233 nm. Lack of additional peaks makes it rather difficult to identify this phase solely based on XRD results.

Fig. 1(b) and (c) show XRD plots for the Ni–25Al films deposited at substrate temperatures of 200°C and 400°C, respectively. In addition to the intensity maximum at $2\theta \approx 44°$, a second peak at $2\theta \approx 51°$ is present in both these diffraction patterns. These two peaks can be consistently indexed as the {111} and {002} peaks of an f.c.c. phase (with or without chemical ordering) with a lattice parameter of $a = 0.356$ nm, which is similar to the lattice parameter of bulk $L1_2$ Ni_3Al. The presence of the {002} diffracted intensity in these two films suggests a loss of texturing with an increase in the deposition temperature. Interestingly, the FWHM of the {111} peak increases for the film deposited at 200°C with respect to the film deposited at ~45°C suggesting a reduction in the average size of the diffracting domain or grain. However, for the film deposited at 400°C, the FWHM reduces with respect to the film deposited at 200°C suggesting grain growth at higher deposition temperatures. The implications of these results will be clear from the TEM observations that have been reported in the subsequent section. The peak at

$2\theta = 39.44°$ is present in the film deposited at 200°C [Fig. 1(b)] but exhibits a relatively lower intensity compared with the equivalent peak from a film deposited at room temperature. This peak is completely absent in the film deposited at 400°C [Fig. 1(c)].

3.2. Transmission Electron Microscopy (TEM)

The microstructure of the Ni–25Al thin film deposited at ambient temperature is shown in the bright field micrograph from a plan-view TEM specimen in Fig. 2(a). The grain size ranges approximately from 30 to 50 nm. Fig. 2(b) is a plan-view selected area diffraction (SAD) pattern from the same specimen. Except for one, all the diffracted intensities could be indexed based on a Ni(Al) f.c.c. phase with a lattice parameter of $a_{f.c.c.} = 0.356$ nm and an h.c.p. phase with a lattice parameter of $a_{h.c.p.} = 0.252$ nm (Table 1). There is no evidence of chemical ordering in either of these two phases due to the lack of any superlattice reflections in the diffraction patterns. Using the {0002} and $\{10\bar{1}0\}$ interplanar spacings, a *c*/*a* ratio of 1.627 was calculated for the h.c.p. Ni(Al) phase. Additionally, a diffracted intensity is observed at an interplanar spacing of ~0.141 nm (refer to Table 1). Coupling the results of the X-ray and electron diffraction studies it is now possible to attribute the diffracted intensities at 0.228 nm (X-ray) and 0.141 nm (electron) to the {111} and {220} planes of an f.c.c. Al-rich solid solution with a lattice parameter of ~0.395 nm. Microdiffraction patterns from two different areas of the plan-view specimen are shown in Fig. 2(c) and 2(d) which can be indexed as the ⟨112⟩ from the f.c.c. phase and ⟨0001⟩ zone axis of the hexagonal phase. In order to determine the location of the f.c.c. Al(Ni) phase in the microstructure, dark field images have been recorded using the diffracted intensity at a *d*-spacing of ~0.141 nm. Fig. 2(e), a dark field micrograph, exhibits a fine dispersion of particles of the Al(Ni) phase within the grains of the matrix. A bright field micrograph from a cross-section specimen of the Ni–25Al film deposited at ambient temperature is shown in Fig. 2(f). The columnar growth morphology is apparent in this micrograph. In addition, a high density of defects parallel to the film/substrate interface is visible within the columnar grains. One of these defects, imaged in high resolution in Fig. 2(g), is identified as a twin on the {111} plane of the f.c.c. phase.

A SAD pattern from a plan-view specimen of the Ni–25Al film grown at a substrate temperature of 200°C is shown in Fig. 3(a). The corresponding bright field micrograph is shown in Fig. 3(b). All the diffracted intensities in the SAD pattern from the 200°C sample can be consistently indexed based on a disordered f.c.c. Ni–25 at% Al phase and the Al rich f.c.c. Al(Ni) solid solution. Table 2 is a list of the interplanar spacings corresponding to these intensity maxima. Based on the XRD pattern [Fig. 1(b)] and the SAD pattern recorded from this thin film, the lattice parameter of the f.c.c. Ni–25Al phase was found to be 0.356 nm which is close to that of bulk $L1_2$ Ni_3Al. An interesting feature of the diffraction pattern from this specimen is that it includes intensities from all possible f.c.c. planes and unlike the film deposited at ambient temperatures, is not restricted to the ⟨111⟩ zone axis. This is in agreement with the XRD pattern that showed the onset of a {200} diffracted intensity in addition to the {111} peak. The microstructure of this film is shown in the bright field micrograph in Fig. 3(b). Interestingly, the average grain size in this film appears to be smaller than that of the film deposited at ambient temperature [Fig. 2(a)] suggesting that recrystallization has occurred. The relatively low diffracted intensity from the f.c.c. Al(Ni) solid solution suggests that the volume fraction of this phase reduces with increasing substrate deposition temperature. This result is consistent with the XRD results (refer Fig. 1).

A SAD pattern and a bright field micrograph from a plan-view specimen of the 400°C sample are shown in Fig. 4(a) and 4(b), respectively. The average grain size in this film (~125 nm) is significantly larger than that observed in the case of the film deposited at 200°C (~15 nm). The ring diffraction pattern [Fig. 4(a)] does not show any diffracted intensities from the f.c.c. Al(Ni) phase. Additionally, the presence of {100} and {110} diffracted intensities in this pattern suggests long-range chemical ordering in the f.c.c. Ni_3Al phase. All the rings can be consistently indexed based on an ordered $L1_2$ Ni_3Al structure. The presence of all

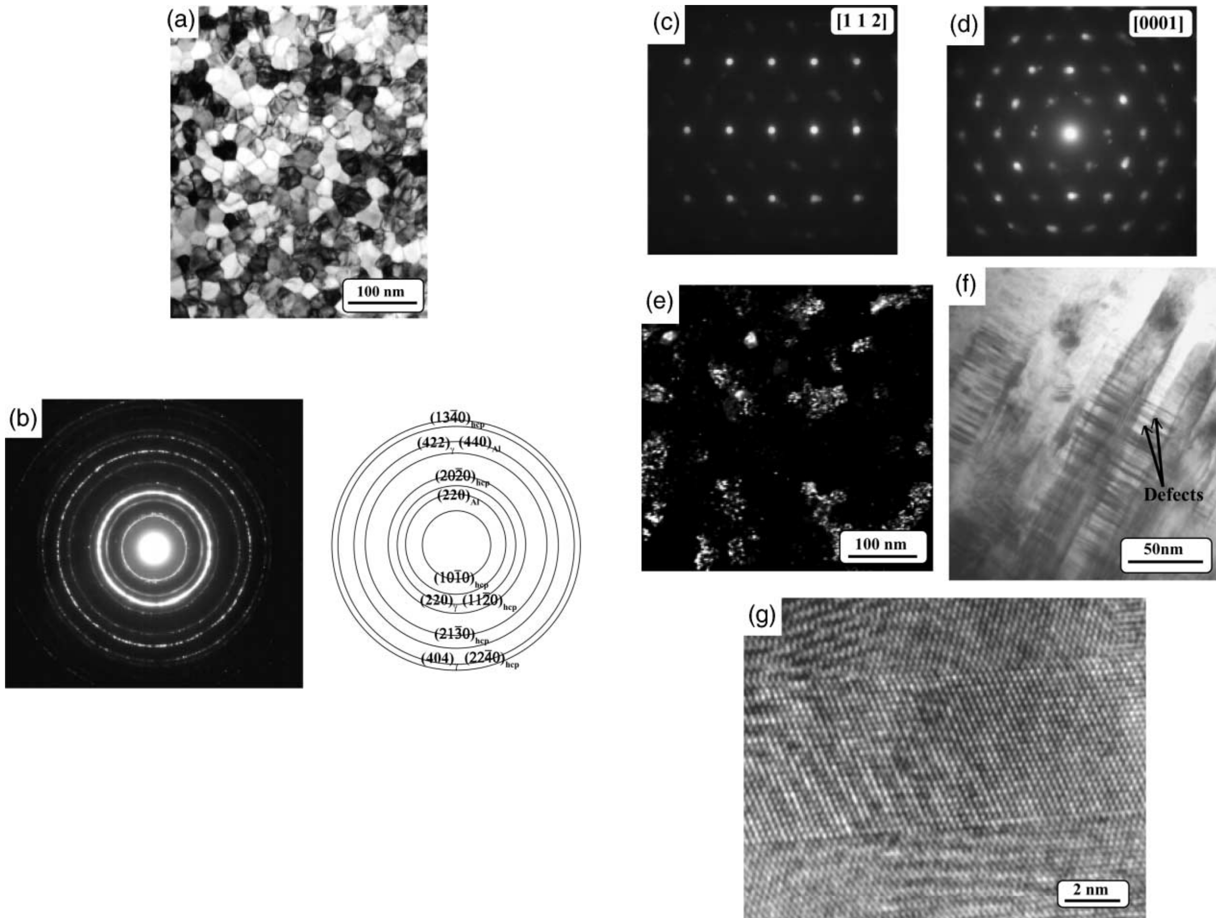

Fig. 2. (a) Bright field plan-view TEM micrograph showing the microstructure of the textured Ni–25Al thin film deposited at ~45°C. (b) Plan-view SAD pattern together with a key figure from the same thin film. The diffracted rings have been indexed based on a disordered f.c.c. Ni(Al) phase, a h.c.p. Ni(Al) phase and an Al rich f.c.c. Al(Ni) phase. (c) $[112]_{f.c.c.}$ zone axis microdiffraction pattern from the f.c.c. Ni(Al) phase in this film. (d) $[0001]_{h.c.p.}$ zone axis microdiffraction pattern from the same film. (e) Dark field TEM micrograph showing the fine dispersion of grains of the Al-rich f.c.c. Al(Ni) phase within grains of the matrix. (f) A cross-section bright field TEM image from the same thin film showing the columnar morphology of grains and the high density of faults parallel to the substrate. (g) A high resolution cross-section TEM micrograph showing the twinned structure of a fault in the same film.

possible $L1_2$ diffracted rings suggests the lack of any significant texturing in this film, similar to the case of the film deposited at 200°C. The interplanar spacings for the diffracted intensities in the SAD pattern recorded from this film are listed in Table 3. The presence of chemical ordering in the Ni_3Al grains is evident from the {110} type superlattice reflections in the [111] zone axis microdiffraction pattern from this phase. This is shown in Fig. 4(c).

4. Discussion

4.1. Constitution of the deposited films

The X-ray diffraction and electron microscopy studies show that the as-deposited films consist of a number of phases. For deposition at ambient temperature, the film with an average composition of Ni–25 at% Al consists of f.c.c. and h.c.p. dis-

Table 1
A table listing the interplanar spacings (*d*-spacings) corresponding to the intensity maxima in the SAD pattern [Fig. 2(a)] from the plan-view specimen of the Ni–25Al thin film deposited at ~45°C. The corresponding indices from the different phases are also listed

d Spacing (nm)	Disordered f.c.c. Ni(Al)	f.c.c. Al(Ni)	h.c.p. Ni(Al)
0.218			$10\bar{1}0$
0.205	111		0002
0.145		220	
0.126	220		$11\bar{2}0$
0.109			$20\bar{2}0$
0.82			$21\bar{3}0$
0.73	422	440	$03\bar{3}0$
0.63	404		$22\bar{4}0$
0.60			$13\bar{4}0$

Table 2
A table listing the *d*-spacings and possible indices for the phases found in the Ni–25Al film deposited at 200°C

d Spacing (nm)	f.c.c. Ni(Al)	f.c.c. Al(Ni)
0.235		111
0.203	111	200
0.176	002	
0.144		220
0.124	220	
0.106	311	
0.102	222	400
0.89	004	
0.81	133	
0.79	204	

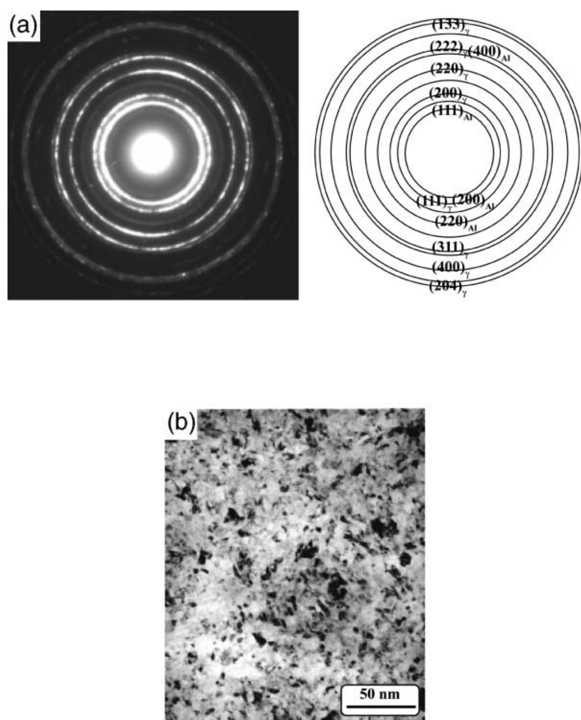

Fig. 3. (a) Plan-view SAD pattern and the corresponding key figure from the Ni–25Al thin film deposited at 200°C. The presence of diffracted intensities such as {002} suggests the lack of a strong ⟨111⟩ in this film. (b) A plan-view bright field TEM micrograph showing the microstructure of this film. Note the smaller average grain size in this film as compared with the film deposited at ~45°C.

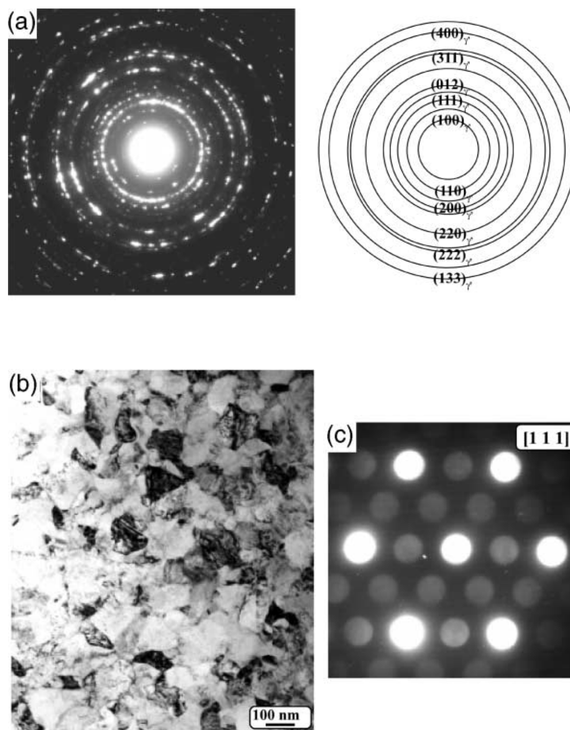

Fig. 4. (a) SAD pattern and corresponding key figure from a plan-view TEM specimen of the Ni–25Al thin film deposited at 400°C. The presence of superlattice reflections such as {100} and {110} is evidence for the ordered nature of this phase. A lack of a strong ⟨111⟩ texture is also evident from the diffraction pattern. (b) Bright field TEM micrograph exhibiting substantially coarser grains in this film as compared with the film deposited at 200°C. (c) A [111] zone axis microdiffraction pattern from a grain in this film exhibiting {110} superlattice reflections of the $L1_2$ structure.

Table 3
A table listing the *d*-spacings and possible indices for the phases found in the Ni–25Al film deposited at 400°C

d Spacing (nm)	$L1_2$ Ni_3Al
0.356	100
0.252	110
0.206	111
0.179	002
0.160	012
0.127	220
0.107	311
0.103	222
0.878	004
0.82	133

ordered phases containing copious defects. The as-deposited films are characterized by a high density of these defects. It is tempting to speculate that a possible explanation for the splitting of the most significant intensity maximum in Fig. 1(a) (at $2\theta \approx 44°$) involves the presence of these two types of stacking sequences, i.e., f.c.c. and h.c.p., where the separation into two peaks might be caused by lattice relaxation of the h.c.p. regions in a direction normal to the surface. In addition, a metastable Al-rich disordered f.c.c. phase has been observed. Since the average film composition is Ni–25Al, the presence of an Al-rich metastable f.c.c. Al(Ni) in the microstructure implies that the compositions of both the f.c.c. and h.c.p. Ni(Al) phases are greater than 75 at% Ni. These results allude to the possibility of a phase separation occurring in the film deposited at ambient temperature [9]. The decrease in the volume fraction of the f.c.c. Al(Ni) phase with increasing deposition temperature is consistent with the metastable nature of this phase, a consequence of the high quench rates involved in sputter deposition. At a deposition temperature of 200°C, the Ni–25Al film consisted largely of disordered f.c.c. Ni(Al), with the exception that small quantities of the Al-rich disordered f.c.c. phase still present. For a deposition temperature of 400°C, the film is entirely ordered $L1_2$ Ni_3Al.

4.2. Recrystallization, texture, and chemical ordering in the Ni–25Al thin films as a function of deposition temperature

The film deposited at ambient temperature exhibited a strong {111} texture in marked contrast to those deposited at higher temperatures. Factors such as anisotropic surface energy, interfacial energy and elastic strain energy or a combination of these are primarily responsible for determining the preferred orientation in thin films [10]. Also, the substrate temperature during deposition influences texture development. Thus, at low substrate deposition temperatures, the mobility of adatoms on the surface is low and therefore textures, even in thick films, are determined in the early stages of deposition during which nucleation plays the most dominant role in determining the film structure. Walton [8] predicted that low substrate temperatures or high rates of deposition favored the alignment of the closest packed planes of the material being deposited parallel to the surface. Therefore, for the case of f.c.c. materials, the preferred texture for low substrate deposition temperatures involves {111} planes being parallel to the surface since the {111} planes are the most densely packed planes in f.c.c.. Indeed, Ni thin films sputter deposited at ambient temperatures on oxidized Si substrates were found to exhibit {111} textures [10]. Since all the Ni–25Al thin films have been grown on oxidized Si substrates with 200 nm amorphous oxide layers on the substrate surface, the substrate is not expected to induce any preferential texture in the film. Therefore, as might be expected the Ni–25Al film deposited at ~45°C is strongly textured with the ⟨111⟩ direction lying parallel to the film normal.

Both in the present study and in the work of Shi et al. [6], elemental Ni films deposited at elevated temperatures (~600°C) were highly textured and exhibited a columnar grain morphology with the grain size being larger than those in films deposited at ambient temperature. These results are in marked contrast to those obtained from deposition of the Ni–25Al films at 200°C and 400°C, respectively. Thus, it is expected that the increased mobility of adatoms on the heated substrates would result in a coarser distribution of columnar grains,

as observed for f.c.c. Ni. Here for the 200°C film the opposite trend is observed, and moreover, the degree of texture is also significantly reduced. It is possible that stresses building up in the thin layer may cause recrystallization in the films deposited at higher temperatures and thus account for these differences in microstructure. However, typical recrystallization temperatures in bulk Ni_3Al are expected to be of the order of $0.5T_m$ (where T_m is the melting temperature of the intermetallic) i.e. ~700°C, which is much higher than the temperatures corresponding to thin film deposition in this study. Thornton's zonal model [11] of elemental metal thin films predicts equiaxed, recrystallized structures at ~0.8 T_m. While there may be some relaxation effects occurring in thin films which may reduce the recrystallization temperature somewhat, it is more probable that some other source of local heating is involved. One possibility involves chemical ordering. Ni_3Al is a strongly ordering compound and consequently the formation of this intermetallic compound is a highly exothermic process with a $\Delta H = -40$ kJ/g−atom [12]. A comparison of Figs. 3(b) and 4(b) indicates grain growth beyond recrystallization in the film deposited at 400°C.

From the characterization of the films deposited at ambient temperature, it appears that during the initial stages of growth of the thin film, columnar grains of a metastable disordered f.c.c. Ni(Al) phase or h.c.p. Ni(Al) phase are formed. Subsequently, if the substrate is unheated, these grains are kinetically constrained from undergoing any phase or structural transformations. In contrast, if the substrate is heated, the enhanced diffusivities allow for atomic rearrangements, required for chemical ordering, to take place. During the process of chemical ordering, a large amount of heat would be evolved causing local heating of the film. Consequently, these regions of the growing film could experience temperatures which are significantly in excess of the substrate temperature and perhaps closer to the recrystallization temperature for this compound. The very fine grain size exhibited in the microstructure of the film deposited at 200°C is consistent with a very short thermal excursion that could occur from short-range ordering of the Ni_3Al. The film deposited at 400°C exhibits a microstructure consisting of slightly coarser grains of fully ordered $L1_2$ Ni_3Al. Presumably, the grain growth and ordering is due to the prolonged exposure at 400°C.

Recrystallization of the films could either lead to randomly oriented grains or a specific recrystallization texture, influenced by a combination of surface energy and strain energy factors. Due to chemical ordering of Ni_3Al, the surface energy anisotropy changes. Atomistic calculations of $L1_2$ ordered Ni_3Al suggest that the value of the interfacial energy, $\gamma(100)$, is dependent on the structure of the termination layer considered [13]. In the case of the $L1_2$ structure, there are two possible terminations of (100) planes possible, a mixed atom termination consisting of both Ni and Al atoms with the ratio Ni:Al = 1:1 and a pure Ni termination. The results of atomistic calculations indicate that for the mixed termination $\gamma_{mix}(100) = 1620$ ergs/cm^2 and for the Ni termination $\gamma_{Ni}(100) = 1885$ ergs/cm^2 [13]. There is only one type of (111) plane in the $L1_2$ structure for which $\gamma(111) = 1645$ ergs/cm^2. Therefore, considering the lower of the (100) surface energies, the ratio of surface energies $\gamma(111)/\gamma_{mix}(100) = \Gamma_{Ni_3Al} = 1.02$. This suggests that the anisotropy in surface energies for chemically ordered Ni_3Al is not very large. Therefore, the recrystallized thin film is not expected to be strongly textured due to the competing influences of the {111} and {002} surface energies. This is in agreement with the X-ray [Fig. 1 (b) and (c)] and the electron [Figs. 3(a) and 4(a)] diffraction patterns from the Ni_3Al thin film deposited at 200°C and 400°C. Note that long range ordering of Ni_3Al was observed only in the case of the film deposited at 400°C as evidenced by the presence of superlattice reflections such as {100} and {110}. However, the finer grain size and lack of strong texture clearly indicates that recrystallization occurred even in the 200°C sample. In previous studies, Okamoto et al. [14] have reported the onset of short range ordering at 150°C and long range ordering at 300°C in disordered f.c.c. Ni_3Al phase. Thus, the recrystallization observed in the 200°C sample presumably occurs due to the onset of short range ordering in this film.

5. Summary

Sputter deposited disordered Ni_3Al thin films were found to be strongly ⟨111⟩ textured when deposited at ambient temperatures on amorphous oxidized Si substrates, the texture being a consequence of the lower surface energy of the {111} planes of the f.c.c. structure. At ambient deposition temperatures, the thin film consisted primarily of a disordered f.c.c. Ni_3Al phases and a small volume fraction of an Al(Ni) phase. Deposition at elevated temperatures (~400°C) resulted in the formation of an ordered $L1_2$ phase in the thin films. For deposition at 200°C and 400°C, ordering of the disordered Ni_3Al phase appears to have caused local heating of the films such that rapid recrystallization occurs consequently reducing the strong ⟨111⟩ texture and developing a finer microstructure.

Acknowledgements

This work was supported in part by the US Air Force Office of Scientific Research, grant number F49620-96-1-0238, Dr. Spencer Wu as Project Manager.

References

[1] Harris SR, Pearson DH, Garland CM, Fultz B. J Mater Res 1991;6:2019.
[2] Kizuka T, Mitarai N, Tanaka N. J Mater Sci 1994;29(21):5599.
[3] Alexander DE, Was GS, Rehn LE. J Appl Phys 1991;69(4):2021.
[4] Eridon JE, Was GS, Rehn LE. J Mater Res 1988;3(4):626.
[5] Cantor B, Cahn RW. Acta Metall 1976;24:845.
[6] Michaelson C, Lucadamo G, Barmak K. J Appl Phys 1996;80(12):6689.
[7] Thompson GB. MS thesis, The Ohio State University, 1997.
[8] Shi Z, Craib GRG, Player MA, Tang CC. Thin Solid Films 1997;304:170.
[9] Banerjee R, Thompson GB, Fraser HL. Philos Mag Lett, submitted for publication.
[10] Walton D. Philos Mag 1962;7:1671.
[11] Thornton JA. Ann Rev Mater Sci 1977;7:239.
[12] American Society for Metals. Selected values of thermodynamic properties of binary alloys, 1970.
[13] Foiles SM, Daw MS. J Mater Res 1987;2(1):5.
[14] Okamoto JK, Ahn CC, Fultz B. J Appl Phys 1995;77(9):4380.